3 Theory

3.1 Introduction

As was discussed in Chapter 2, to model the tensile strength of paper, the following questions must be answered. What are the mechanisms by which the stress transferred from one fibre to other fibres bonded with it? What initiates the macroscopic fracture of paper?

Although numerous studies have been conducted to observe the fracture process of paper, no agreement has been reached as to what initiates the macroscopic fracture of paper. The Page equation (Page 1969) and the KBP model (Kallmes 1977) made a common assumption that the fracture of paper is initiated by the failure of the fibres oriented in the direction of the applied load. The Page equation linked the fibre strength to the zero-span tensile strength of paper by using the second ad hoc premise. The KBP model calculated the sheet strength by making another assumption that paper fails when the sheet strain reaches the failure strain of the fibres. It is clear that both models ignore the load distribution along the axis of a fibre in the sheet, as they used the average load in the fibre to predict the fracture of the paper under stress. Other workers (Van Den Akker 1958; Niskanen 1998) have proposed that it is the failure of the bonds that triggers paper fracture.

In fact, all of the previous analytical models for tensile strength of paper fail to predict the initiation of the fracture of paper. They assumed that all bonds or segments reach the failure threshold simultaneously. This is only true when the sheet is purely homogeneous. In reality, however, the stresses in fibres are not uniform because of the stress transfer. The stress distribution in a fibre in a network will also depend on the local structure of the network.

In section 3.2 of this Chapter, a new simple analytical model for the tensile strength of paper is presented. In the new model, an expression is developed relating paper strength to the stress distribution along the loaded fibres in the paper. This stress distribution function will obviously be determined by the local network structure, including the

positions and nature of the crossing fibres. The new model adopts the assumption made by the Page equation and the KBP model that the fracture of paper is initiated by the failure of the fibres oriented in the direction of the applied load, but considers the load distribution in these fibres. In other words, the local bonding structure of the paper is considered when calculating the paper strength.

In Chapter 8, several attempts are made to fit the theory to the data using stress distributions along the fibre given by different shear lag models. One of the key inputs required in the shear lag models is the distance between the fibre-fibre contacts along the fibre. In section 3.3 a new theory for the number of fibre-fibre contacts in a network will be presented. This theory will be tested against the experimental data in Chapter 7 as well as being used as input for the shear lag calculations in Chapter 8.

3.2 Model for tensile strength of paper

3.2.1 Fibre network model

We consider here a random fibre network with reasonably high density and tensile strength. The plasticity of the network is mainly caused by stretch of the fibres in it. When the fibre network is loaded, the stresses are transferred from one fibre to its adjacent fibres by the mechanism of the form predicted by the shear lag model.

3.2.2 Criteria for fracture

The tensile strength is the maximum load that occurs at the moment that macroscopic rupture begins. Once the rupture has been initiated, it proceeds rapidly during the tensile testing. Therefore, the initiation of the macroscopic fracture of the fibre network is critically important for the tensile strength of paper. We assume that the macroscopic fracture of the fibre network is triggered by the fracture of the most stressed fibre segments in it. The highest stressed fibre segments most likely exist in the fraction of fibres that are oriented in the direction of the applied load. We assume that once the peak load in these fibres exceeds the strength of these fibres, they will break and trigger

the macroscopic fracture of the network. This rupture, once initiated at a point in the sheet, is propagated rapidly in two directions.

3.2.3 Theory

We start with a cross-sectional slice through the sheet taken perpendicular to the stress-direction (See Figure 3-1). For a unit area of the sheet with apparent density, ρ_a, under some stress, σ, then the average stress in the fibre wall, $\sigma_{f,av}$ is

$$\sigma_{f,av} = \frac{\rho}{\rho_a}\sigma \qquad \textbf{3. 1}$$

where ρ is the density of the cell wall material. This equation holds true not matter what the fibre orientation distribution is.

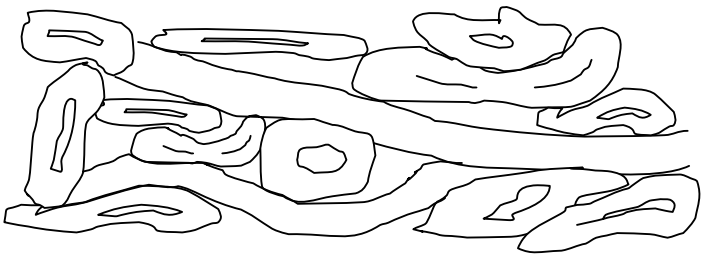

Figure 3-1 Cross-sectional image of the fibre network

Cox's (Cox 1952) result is that for sheets with randomly orientated fibres, the stress in the fibres lying parallel to the loading direction is 3 times larger than if all of the fibres had been aligned with the stress direction. As the fibres that are most heavily loaded are the ones that break first when fracture begins, we consider only the loads on the fibres in the 0^o (parallel to applied stress) position. If we denote these fibres with the superscript, *o*, then

$$\sigma^o_{f,av} = 3\frac{\rho}{\rho_a}\sigma \qquad \textbf{3. 2}$$

Any fibre cutting a sheet cross-section will do so at a random place along the fibre. Accordingly, unless the stress is completely uniformly distributed along the fibre, the actual stress in the fibre at that point will differ from the average. We define the

maximum stress in a fibre as being related to the average stress by a ratio where the value of r will depend on the fibre length and the degree of bonding. Accordingly

$$\sigma^{o}_{f,\max} = 3r\frac{\rho}{\rho_a}\sigma \qquad \textbf{3. 3}$$

If we assume that the fracture of the sample begins when the fibres begin to break and we designate this stress as σ_b, then this must be related to the breaking stress of the fibres, $\sigma_{f,b}$ by

$$\sigma_b = \frac{\sigma_{f,b}\rho_a}{3r\rho} \qquad \textbf{3. 4}$$

3.2.4 Estimation of fibre breaking stress

There are two possible methods of measuring the fibre breaking stress- measuring single fibre strength or measuring the zero-span strength. Measuring the zero-span strength is preferable as in the zero-span test the fibres are measured in the sheet. This is not insignificant, as the mechanical properties of the fibres will depend on how they have been dried. In other words we would not expect that the strength of fibres which have been allowed to freely dry to be the same as fibres which have been dried under restraint in the sheet. The other advantage of the zero-span test is that it is affected by distributions in fibre strength (El-Hosseiny and Bennett 1985). That is, the larger the distribution in fibre strength, the more the zero-span tensile strength will be reduced below the strength based on the expected average. This is also likely to be true for paper tensile strength.

From zero-span theory, for a randomly oriented sheet, the zero-span strength, σ_z, will be 3/8 of the strength measured if all of the fibres had been oriented in the direction of applied stress (Van Den Akker 1958). Therefore Equation 3.4 can be rewritten as:

$$\sigma_b = \frac{1}{r}\frac{\rho_a}{\rho}\frac{8}{9}\sigma_z \qquad \textbf{3. 5}$$

3.2.5 Estimation of r

In the model for tensile strength, r is defined as the ratio of the maximum load to the average load in the fibre. For any axial load distribution, an example of which is shown in Figure 3-2, r is by definition:

$$r = \frac{F_{\max} L}{A} \qquad \textbf{3. 6}$$

Where $F_{\max}$ is the peak axial load in the fibre, L is the length of the fibre and A is area under the load distribution curve that when divided by L is equal to average load in the fibre.

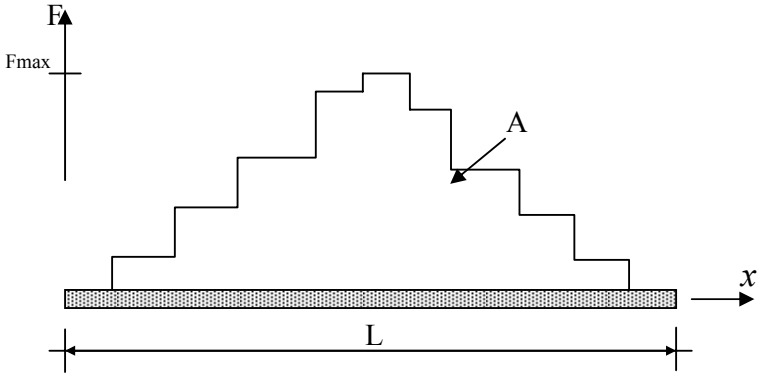

Figure 3-2 Axial force along length of fibre

In general, the value of r is believed to be a function of fibre length and number of fibre-fibre contacts. In the model for tensile strength, Equation 3.5, r describes the efficiency that the paper network uses the strength of the fibres in the paper. Thus although there is no expression for bonded area and fibre length in the expression for the breaking strength of the paper, these will appear in the expression for r.

The problem will be easily solved if the axial load distribution in the fibre is known. Simulation of a fibre network with Finite Element Method (FEM) is believed to be the best way to determine the axial load distribution in the fibre, provided the network is simulated in sufficient detail. However, it is impossible to do such a simulation in this project due to the limited time range.

As a start for estimating the value of r, we will use the shear lag model to analyse the stress distribution along the axis of a fibre. The shear lag model (Cox 1952), as discussed in Chapter 2, predicts that stress is transferred from each fibre to its adjacent fibres in the regions of the fibre ends. The stress in a fibre is at its maximum at the center and diminishes to zero at the ends. The application of the shear-lag model and other methods to determine r is discussed in Chapter 8.

3.3 Model for number of fibre-fibre contacts and expressions for relative bonded area (*RBA*)

As discussed above, a model for number of fibre-fibre contacts in paper is required for determination of the value of r in the new model for tensile strength of paper (Equation 3.5).

Fibre-fibre contacts have long been an interesting topic in the study of paper physics with numerous attempts to develop analytical models for the number of fibre-fibre contacts. Corte and Kallmes (Corte 1962) presented the first important model for number of fibre crossings in a three dimensional random fibre network. An expression equivalent to this model was proposed some years later by Komori and Makishima (Komori and Makishima 1977). Komori and Makishima's model was later modified by Pan (Pan 1993) by allowing for the reduction in free fibre length due to existing contacts. Pan's work was criticized and corrected by Komori and Itoh (Komori and Itoh 1994). Later a similar model was also derived independently by Dodson (Dodson 1996). More recently Dent (Dent 2001) showed that the 'general gamma' distribution can statistically describe 'non-random' as well as 'random' structures. These models use statistical analysis to predict the possible number of fibre-fibre contacts that a certain number of fibres could make in a given volume. They ignore the effects of fibre cross-sectional properties on the fibre-fibre contacts, so cannot model the effects of fibre collapse. In fact, however, the fibre width, fibre height and the fibre collapse degree all affect the fibre-fibre contacts. It is necessary to include these parameters in any model of fibre-fibre contacts.

Because the measurement of the number of fibre-fibre contacts is usually very difficult, it has always been problematic to obtain effective data to verify different models for the number of fibre-fibre contacts. In this subsection, we first present a new analytical model for the number of fibre-fibre contacts, which relates the cross-sectional properties of the fibres in the sheet to the number of fibre-fibre contacts per unit length of fibre. The model is further used to derive expressions for the Relative Bonded Area (*RBA*) for the purpose of verifying the model for number of fibre-fibre contacts by using data of *RBA*.

3.4 The new model for number of fibre-fibre contacts

3.4.1 Model paper structure

We start with the model fibre cross-section shown in Figure 3-3. A fill factor, f_h, is defined as the ratio of the fibre wall area, A_f, to the area of the smallest rectangular bounding box, A_b, that can completely enclose the irregular shape of the fibre and with its one side parallel to the paper plane. Here D_h and D_w are the minimum dimensions of the rectangular bounding box.

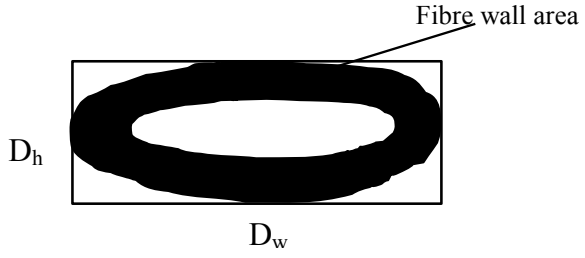

Figure 3-3 The bounding box surrounding a model fibre

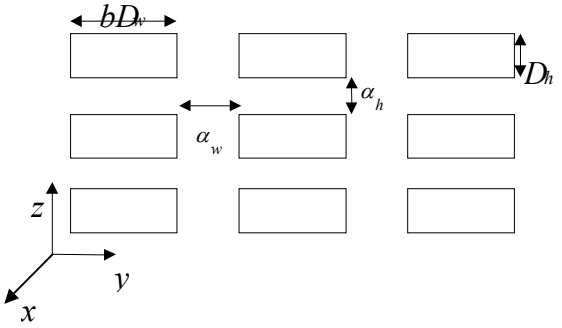

Figure 3-4 Idealized cross-sectional matrix of fibres

A paper sheet cross-section is then idealized as a regular matrix as shown in Figure 3-4, in which only the bounding boxes of the fibres are shown. The factor, b, here is an angle factor and accounts for the fibres in general not cutting the $y-z$ plane at right angles. In the situation depicted, z is the direction through the sheet thickness and the y axis can be selected to be any direction within the plane of the sheet. The apparent density of the sheet, ρ_a, is (ignoring the effect of surfaces)

$$\rho_a = \frac{\rho f_h D_h b D_w}{(D_h + \alpha_h)(bD_w + \alpha_w)} \qquad \textbf{3. 7}$$

where ρ is the density of the cell wall material, and α_h and α_w are the packing variables giving the spacing of the fibres within each layer and between the layers, respectively. In this equation, f_h, D_h and D_w can be relatively readily determined by confocal microscopy, leaving b, α_w and α_h to be estimated theoretically.

3.4.2 Determination of b, α_w and α_h

To determine b, we need to determine the average angle that a fibre makes in crossing the *y*-axis. If the distribution of fibre angle is random (as in a standard handsheet) then the average angle to any given plane perpendicular to the *x*-axis is:

$$\theta_{av} = \frac{\int_0^{\pi/2} \theta \cos\theta \; d\theta}{\int_0^{\pi/2} \cos\theta \; d\theta} \qquad \textbf{3. 8}$$

Here the factor $\cos\theta$ is the probability density function for the number of fibres having angle θ to any given plane. For a sheet with random fibre orientation, the theoretical value of θ_{av} given by Equation 3.8 is $\pi/2-1$, or 32.7°. Equation 3.8 could be made general for a machine made paper by replacing $\cos\theta$ with a function $F(\theta)$, which would include the distribution information. The value of b is then given by $b = 1/\cos\theta_{av}$.

The idealized matrix presented in the previous section represents the fibres sitting in their idealized positions and not actually in contact with each other. Letting Figure 3-5 and Figure 3-6 depict the idealized *x-y* and *x-z* models, then $2\Delta L$ is the distance along the fibre axis between the fibre crossing midpoints and from geometry the following relationship can be derived.

$$\sin\theta_{av} = \frac{\alpha_w + aD_w}{2\Delta L} \qquad \textbf{3. 9}$$

The layer-layer separation is determined by α_h. Figure 3-6 shows fibres within a single layer crossing each other. As a strong theoretical basis for determining layer-layer separation is lacking, we assumed that $\alpha_h = \beta D_h$. Here β is a packing factor that will be determined experimentally.

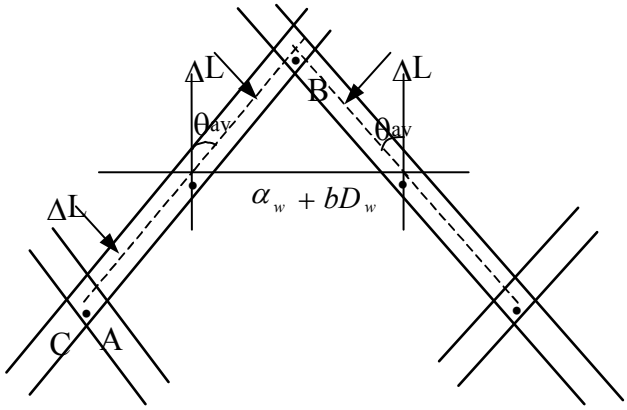

Figure 3-5 Fibre-Fibre crossing within a layer (*x-y* Projection)

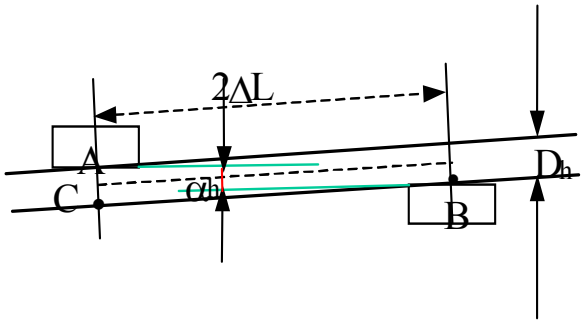

Figure 3-6 Side view of fibre-fibre contacts in one layer (x-z Projection)

3.4.3 Apparent density and Number of fibre-fibre contacts

Substituting the expressions for b, α_h and α_w into Equation 3.9, we obtain the following expression for the apparent density:

$$\rho_a = \frac{\rho f_h D_w}{(1+\beta)\Delta L \sin 2\theta_{av}} \qquad \textbf{3. 10}$$

Now if we assume that an equal number of fibre-fibre contacts on a fibre come from the layers above and below a given layer then the number of fibre-fibre contacts per unit length of fibre, N_c is given by:

$$N_c = \frac{3(1+\beta)}{2}\frac{\rho_a}{\rho f_h}\frac{\sin 2\theta_{av}}{D_w} \qquad \textbf{3. 11}$$

There is very little data that can be used to check the validity of this expression. One such set of data is the work of Elias (Elias 1967) in which data was obtained for the number of contacts per mm of fibre length for mats of glass fibres with a diameter of 7.22 μm and varying lengths, that were pressed at different pressures. When this data was taken into Equation 3.11, β was found to be –0.6, as shown in Table 2-1. The value of β is negative meaning that fibres from any given layer have deflected up and down into its neighbouring layers.

Table 3-1 Calculated value of β by Equation 3.11 using Elias' data

Fibre length (mm)	Diameter (μm)	Mean No. contacts per mm	Solid fraction	Calculated value of β
2.26	7.22	3.2	0.0310	-0.57
2.26	7.22	5.0	0.0488	-0.57
2.26	7.22	5.6	0.0545	-0.57
1.09	7.22	6	0.0739	-0.66
4.55	7.22	4.7	0.0575	-0.66

*For the cylindrical glass fibres, the fill factor, f, is given by $\pi/4$.

The fact that the calculated value of β is approximately constant is an important indicator that Equation 3.11 could provide an accurate predictor of the number of fibre-fibre contacts.

3.5 Expressions for *RBA*

Equation 3.11 can be used to provide theoretical expressions for the RBA. Two different expressions for the RBA were given in consideration of the two different methods used for RBA determination.

If the RBA is measured by nitrogen adsorption, then the total surface area of a unit length of fibre can be assumed to be $2(D_w + D_h)$. If the area of each fibre contact is A_c, then the Relative Bonded Area for nitrogen adsorption, RBA_{N_2}, can be written as:

$$RBA_{N_2} = \frac{N_c A_c}{2(D_w + D_h)} \qquad \textbf{3. 12}$$

One critical assumption is that the sheets are thick enough so that the exclusion of the effect of the surfaces of the sheet from this calculation does not introduce significant error. The second critical assumption is that if the fibres are purely ribbon-like, the projected area of each contact may be expressed as $A_c = D_w^2/\sin 2\theta_{av}$. However, in a real sheet, the actual area of each contact could differ from the idealized situation of two rectangles with width, D_w, therefore a factor, R, should be taken into account for

calculating A_c i.e. $A_c = R(D_w^2 / \sin 2\theta_{av})$. When this is substituted in Equation 3.12 together with the expression for N_c from Equation 3.11 then we obtain

$$RBA_{N_2} = \frac{3(1+\beta)}{2}\frac{R}{2}\frac{1}{(1+\delta)}\frac{\rho_a}{\rho f_h} \qquad \textbf{3. 13}$$

in which $\delta = D_h / D_w$.

For the *RBA* measured by scattering coefficient we assume that only the top and bottom surfaces contribute to the measured scattering coefficient, from which it can be shown that

$$RBA_{sc} = \frac{3(1+\beta)}{2}\frac{R}{2}\frac{\rho_a}{\rho f_h} \qquad \textbf{3. 14}$$

The model for number of fibre-fibre contacts presented in this chapter can be validated directly with data for number of fibre-fibre contacts measured in paper, and can also be validated indirectly with data for *RBA* measured by nitrogen adsorption method and by scattering coefficient method. Techniques for measuring the number of fibre-fibre contacts directly in paper and for measuring the *RBA* are required. A new microscopic technique for quantitative analysis of paper structure at the fibre level has been developed and validated and is presented in Chapter 6. Based on this new technique, technique for measuring the fibre-fibre contacts directly in paper has also been developed. This is discussed in Chapter 7. These new techniques together with new techniques for measuring the *RBA* that has been developed in this project are then used for obtaining data for validation of the new model for number of fibre-fibre contacts in paper. This is discussed in Chapter 8.

3.6 Summary

This chapter has presented a new analytical model for tensile strength of paper based on the assumption that the macroscopic fracture of paper is trigger by the failure of fibres lying in the direction of the applied load. The new model relates the tensile strength to the zero-span strength of the component fibres through a factor r. The sheet density only comes in as the equation are derived for stresses and not as tensile index. In other words it corrects for the void volume in the sheet. The value of r is the ratio of the peak load and the average load in the fibres, and r is believed to be a function of

number of fibre-fibre contacts and fibre length. It is the first analytical model that attempts to predict the start point of paper failure under load.

A new model that relates the fibre cross-sectional dimensions and the apparent density of paper to the number of fibre-fibre contact per unit length of fibre has been presented in this chapter. It is the first model that considers the effects of fibre cross-sections on the fibre-fibre contacts.

The model for number of fibre-fibre contacts will be fully verified in Chapter 7. The experimental verification for the model for tensile strength of paper will be presented in Chapter 8.